Cold-neutron depth profiling as a research tool for the study of surface oxides on metals

Tun, Z.; Noël, J. J.; Bohdanowicz, Th.; Cao, L. R.; Downing, R. G.; Goncharova, L. V.

Publisher's version / Version de l'éditeur:
https://doi.org/10.1139/P10-062
Canadian Journal of Physics, 88, 10, pp. 751-758, 2010-10-01

Cold-neutron depth profiling as a research tool for the study of surface oxides on metals[1]

Z. Tun, J.J. Noël, Th. Bohdanowicz, L.R. Cao, R.G. Downing, and L.V. Goncharova

Abstract: A recent experiment at NIST has demonstrated that neutron depth profiling (NDP) based on the (n, α) reaction could be developed into a tool that could be routinely used for the study of passive oxides on metals. Whereas most metals are not (n, α) active, oxides grown with ^{17}O, the only (n, α) active oxygen isotope, can be observed and tracked by this technique. Problems due to contamination of the samples by boron were encountered, but were shown to be surmountable. For our samples, the NDP facility at NIST, as it exists today, has enough flux and energy resolution to separate the α particles emitted by ^{17}O from those emitted by ^{10}B. Substantial improvement in the data collection rate, easily achievable with arrays of additional detectors, will make NDP a useful tool in the study of passive oxides.

PACS Nos: 61.72.S–, 81.70.Jb, 68.47.De, 68.35.bd, 82.45.Bb

Résumé : Une expérience récente au NIST a démontré que le profilage en profondeur par neutrons (NDP), basé sur la réaction (n, α), peut devenir un outil d'utilisation courante pour étudier les oxydes passifs à la surface des métaux. Alors que la plupart des métaux n'ont pas d'activité (n, α), les oxydes avec ^{17}O, le seul isotope d'oxygène actif (n, α), peuvent être observés et étudiés à l'aide de cette technique. Nous avons eu des problèmes de contamination des échantillons par du bore, mais ils se sont avérés surmontables. Pour nos échantillons, le montage NDP au NIST, tel qu'il existe présentement, a un flux et une résolution en énergie qui sont suffisants pour isoler les α du ^{17}O de ceux du ^{10}B. Une amélioration substantielle du taux de collecte des données, facilement atteignable avec des réseaux additionnels de détecteurs, fera de NDP un outil utile dans l'étude des oxydes passifs.

[Traduit par la Rédaction]

1. Introduction

Passive oxides that grow naturally on the surface of most metals, with the noted exceptions of gold and platinum, are important for the survival of the metals in our O_2-containing atmosphere. Although typically only a few nanometres thick, the oxide layer is key for corrosion prevention. Consequently, there is a continuing need to develop experimental techniques to study oxide layers on metals. We are particularly interested in a technique that would allow us to follow the migration of O atoms as surface reactions modify the protective oxide. Ideally, we would like the technique to be applicable to thin-film samples or metal plates of finite thickness.

The need for such a technique first came to our attention about 10 years ago when we studied the growth of anodic oxide on Ti with neutron reflectometry [1]. As new oxide grew with oxygen ions derived from an aqueous solution, a small amount of hydrogen was found to be incorporated into the oxide layer and remained adjacent to the oxide–water interface. Whether the H remains attached to its companion O, i.e., as an OH ion, or if the ion dissociates once inside the oxide layer is unknown. Whether the original air-grown oxide simply acts as a passive screen as oxygen and metal ions move through it in opposite directions during anodization (the so-called field-assisted ion transport), or if it plays an active part as the ions hop from site to site (point defect model) is also unknown. The reader may wish to see the pictorial representations of these ion transport models in the article "Stop that corrosion, if you can" in a special issue of Physics in Canada [2].

One way of unambiguously answering the questions above is to isotopically label the O atoms and follow the anodic process step by step with a suitable experimental technique. Neutron scattering is not an option since scattering cross-sections of all three O isotopes are very similar. Standard ion beam analysis techniques such as Rutherford back-scattering (RBS), medium energy ion scattering (MEIS), or nuclear reaction analysis (NRA) are isotopically

Received 19 April 2010. Accepted 26 August 2010. Published on the NRC Research Press Web site at cjp.nrc.ca on 7 October 2010.

Z. Tun.[2] Canadian Neutron Beam Centre, National Research Council Canada, Chalk River, ON K0J 1J0, Canada.
J.J. Noël. Department of Chemistry, University of Western Ontario, London, ON N6A 5B7, Canada.
Th. Bohdanowicz. Canadian Neutron Beam Centre, National Research Council Canada, Chalk River, ON K0J 1J0, Canada; Nanotechnology Engineering Undergraduate Program, University of Waterloo, Waterloo, ON N2L 3G1, Canada.
L.R. Cao. Inorganic Chemical Metrology Group, Analytical Chemistry Division, NIST, 100 Bureau Drive, Gaithersburg, MD 20899-8395, USA; Department. of Mechanical Engineering, Ohio State University, Scott Laboratory, 201 W 19th Avenue, Columbus, OH 43210-1142, USA.
R.G. Downing. Inorganic Chemical Metrology Group, Analytical Chemistry Division, NIST, 100 Bureau Drive, Gaithersburg, MD 20899-8395, USA.
L.V. Goncharova. Department of Physics and Astronomy, University of Western Ontario, London, ON N6A 3K7, Canada.

[1]Special Issue on Neutron Scattering in Canada.
[2]Corresponding author (e-mail: zin.tun@nrc-cnrc.gc.ca).

sensitive for oxygen. However, they all suffer from one limitation or another. In general, RBS has good sensitivity to high-Z elements in or on low-Z substrates, but poor sensitivity to low-Z elements, such as oxygen isotopes, on high-Z substrates. If the sample is a millimetre-thick plate electrode, in RBS or MEIS, ions that are backscattered from the polycrystalline metal substrate lead to a very high background, obscuring the weak oxygen signal. Depth resolution for backscattering is limited at higher energies by the energy loss factor, and at lower energies by increased energy straggling. On the other hand, NRA is sensitive to all oxygen isotopes using the $^{18}O(p, \alpha)^{15}N$ and $^{16}O(^3He, p)^{18}F$ or $^{16}O(^3He, \alpha)^{15}O$ reaction, but it has limited depth resolution unless a less common resonant depth profiling is applied. Therefore, these techniques generally work best with thin-film samples prepared on specially selected substrates. One method that holds the promise of being free of such limitations is depth profiling of ^{17}O via the (n, α) reaction. We hereby report a preliminary work carried out to assess this possibility in the study of anodic oxides. Unlike RBS or NRA, this method should lead to a clean signal once practical issues are overcome. It will be applicable to thin-films as well as to plate samples.

2. Principle of neutron depth profiling

Neutron depth profiling (NDP) is a nondestructive technique capable of determining isotopic concentration versus depth distribution in the near-surface region. Profiling to a depth of a few tens of micrometers is possible, with the resolution varying from a few tens of nanometers to a few tenths of a micrometer [3]. It is based on the T(n, α)R reaction, where a neutron (n) reacts with a target nucleus (T) to yield an α particle (or a proton for certain T) and a recoiling nucleus (R). For low-energy neutrons, the reaction is possible only for a few nuclei. As the reaction cross-section is inversely proportional to incident neutron velocity, the detection limit increases for low-energy neutrons, i.e., cold-neutron beams. When cold neutrons are used, the technique is sometimes called cold-neutron depth profiling (CNDP). Interested readers are referred to ref. 3 for more details.

Being a nuclear reaction, the Q-value of the (n, α) reaction is typically a few MeV, while the incident neutron carries only a few meV. This nine orders of magnitude in energy difference has two important consequences: first, the neutron energy is so small as to not dislodge T from its initial reaction site, assuring the depth profile obtained is that of the unperturbed distribution of T; second, all available energy in the final state practically comes from the Q-value, a well-defined quantity. Both the α particle and the recoiling nucleus R emerge from the reaction with known kinetic energies. When these particles are counted with energy-resolving detectors, the values predicted from the Q-value serve as upper limits. Lower energies could be seen if the particles lose energy while traveling from the reaction site to the detector. The energy loss is a measure of the path length traveled by the particle within the sample material before it emerges into the surrounding space (usually vacuum), where the detectors are situated. In the rare case of all nuclei T being localized on the sample surface, a sharp peak with no energy loss would be observed, broadened only by the finite energy resolution of the detector system. In all other cases, the particle count would have components appearing tending to lower energies. The extent of the downward shift from full energy is a measure proportional to depth of the reaction site, and the number of counts at that energy is proportional to the abundance at the corresponding depth. If we know roughly the atomic composition and density of the sub-surface region of the sample, the measured energy loss can be quantitatively related to depth. NDP is therefore a near-surface analytical technique that is very specific to certain isotopes.

The extremely rare isotope of oxygen, ^{17}O, is (n, α) active. Unfortunately, the reaction cross-section for ^{17}O, at only σ_a = 0.236 barns, makes it challenging to collect statistically meaningful spectra without the use of high neutron beam currents and good detection efficiency. On the other hand, elemental boron (20% ^{10}B and 80% ^{11}B) has both a large natural abundance and exhibits one of the largest (n, α) cross-sections, σ_a = 767 barns. Being a very common and mobile element in the environment, boron contamination could seriously jeopardize measurements for ^{17}O. The (n, α) active isotope of boron, ^{10}B, exhibits *two* (n, α) reactions with branching ratios of 94% and 6%. Unfortunately for us, the emission energy of the α particle of the more probable branch is only slightly higher than that of the α particle from ^{17}O. Avoidance of boron contamination is therefore crucial: even a small amount of sub-surface boron, whose α-peak is down-shifted in energy, will completely obscure the intrinsically weak ^{17}O signal. Table 1 shows this disparity very clearly, along with the details of the reactions that are likely to be needed in interpreting our experimental results.

3. Samples and experiment

In spite of our intention to develop a technique that could be used on a plate electrode, we chose to carry out the feasibility study on a thin-film sample because of the practical issues one would encounter in preparing a fresh metal surface of a plate sample. Our samples were thin-films of metallic Ti, sputter-deposited to a thickness of ~50 nm on polished Si substrates (N-type), while maintaining the substrate temperature at 225 °C. Two samples were prepared for NDP, one with the Ti metal surface passivated with a ^{17}O oxide layer and the other passivated with regular oxygen (i.e., natural isotopic abundance of 99.76% ^{16}O). Because of this difference, it was necessary to prepare the two samples separately, but care was taken to keep all experimental parameters as similar as possible. Three additional samples were also made for checking the layer thicknesses with X-ray reflectometry, which led to an estimate of 49 ± 3 nm for the metal layer. Directly measuring thickness on the NDP samples was avoided, since we wished to keep them under a controlled atmosphere as long as possible.

The 100 mm diameter Si substrates for NDP samples were derived from the same fabrication batch (n-type Prime grade wafers from Wafer World, Inc.), and the metal deposition was performed one immediately after the other.[3] At

[3] Certain commercial products are identified in this paper in order to specify the experimental procedures in adequate detail. This identification does not imply recommendation or endorsement by the authors or by the National Institute of Standards and Technology, nor does it imply that the products identified are necessarily the best available for the purpose. Contributions of the National Institute of Standards and Technology are not subject to copyright.

Table 1. Selected physical and nuclear properties for boron, nitrogen, and oxygen (source: ref. 3).

Atomic No.	Element	Reaction	Cross-section (barns)	Isotopic abundance (atom ratio)	Recoil mass energy (keV)	Particle energy (keV)	Branching ratio
5	B	$^{10}B(n,\alpha)^{7}Li$	3837	0.199	1013.126	1775.868	6.28%
5	B[a]	$^{10}B(n,\alpha)^{7}Li$	3837	0.199	839.635	1471.763	93.70%
7	N	$^{14}N(n,p)^{14}C$	1.83	0.99634	42.02	583.851	
8	O	$^{17}O(n,\alpha)^{14}C$	0.236	3.80×10^{-4}	404.064	1413.632	

[a]There is a 477.595 (3) keV γ-ray emission in the 93.7% ^{10}B branch of reactions.

the time of the deposition, the sputtering target (99.9% Ti by American Elements) had already been used to prepare several other samples and had remained in low pressure Ar atmosphere for several days. This was possible because the sputtering chamber was equipped with a load-lock chamber. Subsequent to Ti deposition, each sample was removed through the load-lock chamber into a special container that was also under a dry Ar atmosphere, but at atmospheric pressure. In the first container was a glass ampoule of ^{17}O water (90% enriched ^{17}O water by isoSolutions), and the second container held a similar ampoule with ordinary deionized water. The lids of the ampoules were opened immediately after placement of each Ti sample to initiate oxide growth by introducing water vapour into the Ar atmosphere at ambient laboratory temperature. This sample preparation preceded the neutron experiment by 5 months. Within the first few days, the ampoules were found to have gone completely dry, loading the originally dry Ar with water vapour. Given that we started with $\sim$1 mL of liquid and the volume of each container was $\sim$800 mL, the water vapour content was far from saturation, but we estimated that enough molecules were present in each container to grow passive oxides on as many as 10 000 similar samples. Although being very wasteful of the ^{17}O isotope, the advantage of growing oxide from vapour is that it reduces the chance of contamination by boron. The liquid water may have liberated boron from the surface of the wafer container. At the time of the experiment, the passive oxide on our samples was expected to be $\sim$5 nm thick TiO_2, the typical thickness reached by air-grown oxide in five months [4].

The NDP samples, kept in the Ar atmosphere at all times after metal deposition, were loaded in the NDP chamber at NIST through ambient air. Exposure to ambient air was for about 15 min during mounting and pump-down of the NDP vacuum chamber. No additional oxide should have grown within this brief period; however, even if it did, a few tenths of a nanometer of the air-grown ^{16}O oxide covering the ^{17}O oxide would not affect our study.

Figure 1 shows schematically how the components of the experiment were arranged in the NDP vacuum chamber. The cross-sectional area of the incoming cold-neutron beam was $\sim$2 cm^2, while the active areas of the solid-state detectors were 150 and 100 mm^2. These detectors, referred to as CNDAT and CNBACK, respectively, detected and determined all charged particles derived from the (n, α) reaction, i.e., both the α and recoiling nucleus, that intercept the detectors. As the detectors were situated slightly more than 10 cm from the neutron beam-spot on the sample, the trajectory of the detected charged particles is known to within <5° full width at half-maximum (FWHM).

A calibration immediately prior to our experiment had individually established the energy scales for CNDAT and CNBACK, as well as determined the FWHM energy resolution of 18 and 19 keV, respectively, for the detectors. As explained earlier, observed α particle energy can be related to the path length traveled through the sample material and accordingly the depth of the neutron reaction. For CNDAT, the depth of the reaction site (i.e., the location of ^{17}O or ^{10}B that gives off the α particle) is simply the path length. For CNBACK, due to the 42° viewing angle (see Fig. 1), the path length is approximately the depth times $\sqrt{2}$.

Fig. 1. Schematic of the cold-neutron depth profiling facility at NIST (plan view).

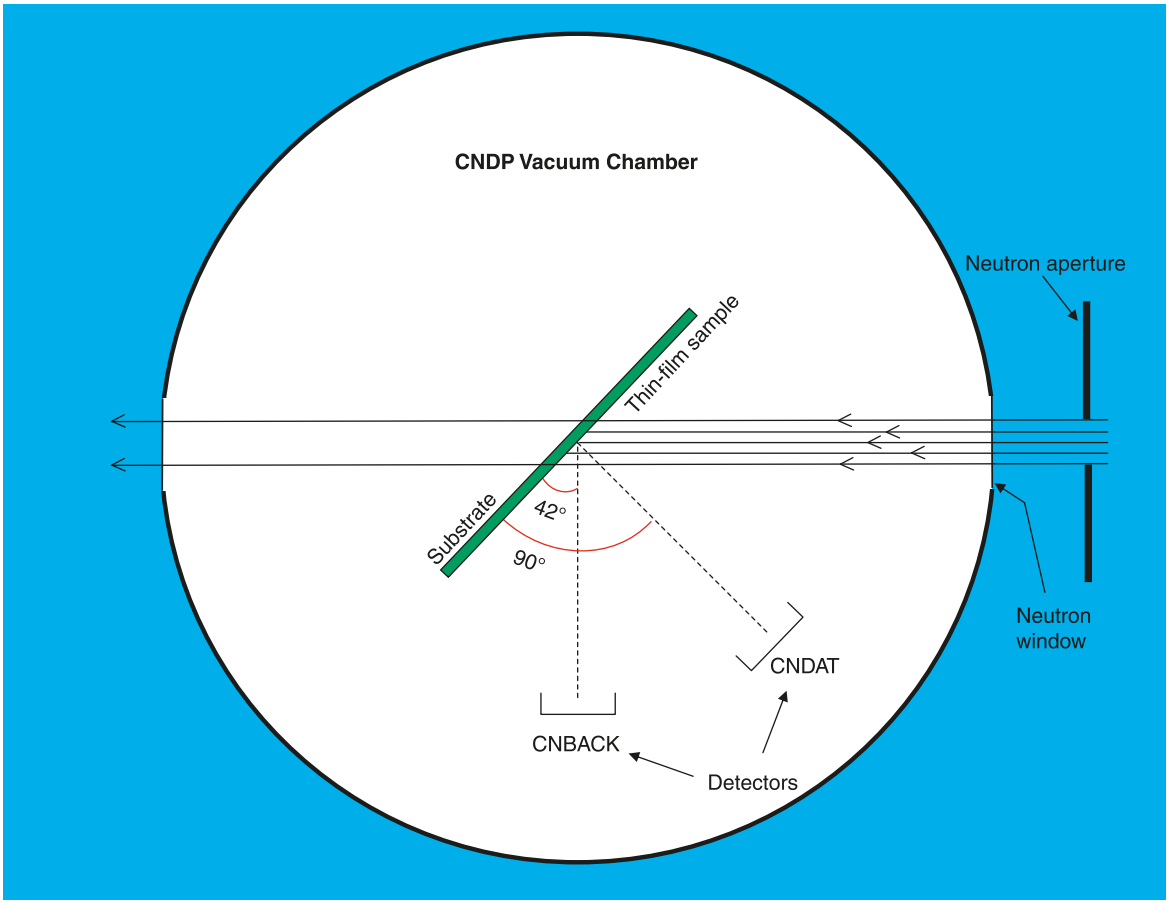

4. Results

The charged-particle spectra obtained by the two detectors are in agreement within counting statistics. Therefore, we will only show the spectra taken by CNDAT. Results from the other detector, CNBACK, will be commented on where they matter significantly to the discussion.

Figures 2 and 3 show the total counts collected by CNDAT over counting periods of 31.00 and 21.93 h, respectively, for the ^{16}O and ^{17}O oxide samples. Vertical lines in the figures mark the channels corresponding to full energies of α-from-O, α-from-B, and the recoil mass, Li-from-B. The full energy of C, recoil mass from the (n, α) reaction of ^{17}O, is very low and outside the range of the plot. We immediately see evidence of boron contamination in both samples, signaled not only by α particles but also by recoiling Li. Based on a comparison with the standard used for energy calibration, we estimate the amount of ^{10}B in the ^{16}O sample (Fig. 2) to be 4.0×10^{11} atoms within the beam footprint and 9.8×10^{11} atoms for the ^{17}O sample (Fig. 3). This appreciable sample to sample variation suggests that we are dealing with a poorly controlled contaminant. Based on the relatively small down-shift from the full energy position (channel 2117, or 1472 keV), the contamination seems to be limited to the titanium region of the samples and not in the silicon region. We will return later to this point when the data are analyzed quantitatively. The important observation here, visible simply by comparing the two figures, is that Fig. 3 contains an extra peak centered at channel 2034, weak in intensity but well-separated from the α-from-B peak. From its position, the lower energy peak can be tentatively attributed to α particles from ^{17}O. The same comparison with the standard as was done for boron, after adjusting the cross-sectional difference, gives an estimate of 1.86×10^{15} of ^{17}O atoms in the beam footprint. The alternative interpretation would be that the sample is contaminated by boron with an enhanced concentration at a particular depth, giving rise to a double-peak feature. Quantitative analysis presented later will show this interpretation to be unlikely.

After the data shown in Fig. 3 were collected, the ^{17}O sample was subjected to anodization by a series of increasing voltages and then loaded back into the NDP chamber for further data collection. Figure 4 is the spectrum of the sample anodized to 4 V (with respect to a saturated calomel electrode), collected over a counting period of 15.22 h. The perception of weaker peaks is the result of a shorter counting time; indeed, the peaks in Figs. 3 and 4 would be of similar strength if the counting time difference was adjusted. For the now anodized ^{17}O sample, we still see the double peak. Re-plotting the data on an expanded energy scale (not shown) suggests that the double peak has shifted slightly down in energy, but limited counting statistics make it difficult to be certain. Our attempt to verify the shift by least-squares fitting was highly subjective, as convergence could be obtained only by introducing constraints. As a more ob-

Fig. 2. Particle spectrum recorded by the CNDAT detector for the Ti thin-film sample covered with ^{16}O oxide. For α particles, the range plotted corresponds to 695.3 to 1807.5 keV. Vertical lines mark the channels where either the α or Li nuclei (as labelled) will appear if the particles escape the sample without losing energy. Channel versus energy calibration for Li is different from that for α particles, and this difference has been taken into account in placing the Li-from-B markers.

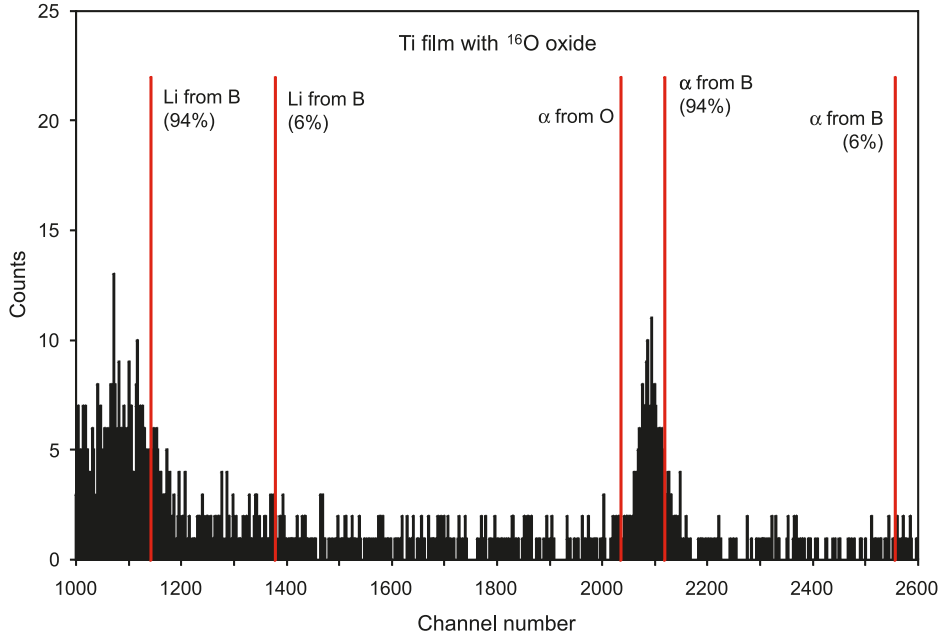

Fig. 3. Particle spectrum as recorded by the CNDAT detector for the Ti thin-film sample covered with ^{17}O oxide.

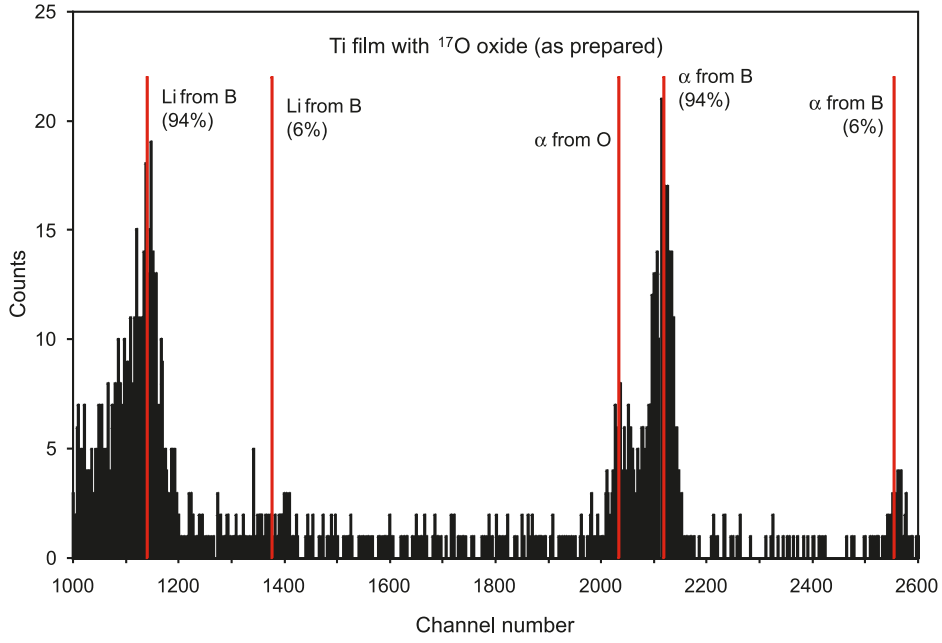

jective approach, we calculated the first moment of counts in the neighbourhood of the double peak. For the range of channels 1950 to 2200 inclusive, the moment of counts is at channel 2093 for Fig. 3 and at channel 2084 for Fig. 4, a shift of 9 channels. In energy, the shift is from 1457.2 to 1451.3 keV, or a 6 keV shift.

A similar shift occurs for the double-peak feature detected by CNBAK. In this case, the moment changes from 1450.8 to 1441.0 keV, a shift of 9 keV, or $\sqrt{2}$ times larger, as expected, than the shift detected by CNDAT. Consistency between the two detectors confirms that the shifts discerned by the moment calculation are not artifacts but are due to anodization, demonstrating that NDP is capable of detecting deeper burial of the α source when the sample is anodized. The only remaining issue now is to revisit the origin of the lower energy component of the double-peak feature.

The strongest evidence for the detection of α emission from ^{17}O (in both Figs. 3 and 4) comes from simulations. For a 49 nm thick Ti film deposited on a silicon substrate and covered by 5 nm layer of TiO_2, the α energy spectra

Fig. 4. Particle spectrum ecorded by the CNDAT detector after the ^{17}O oxide sample is anodized to 4 V.

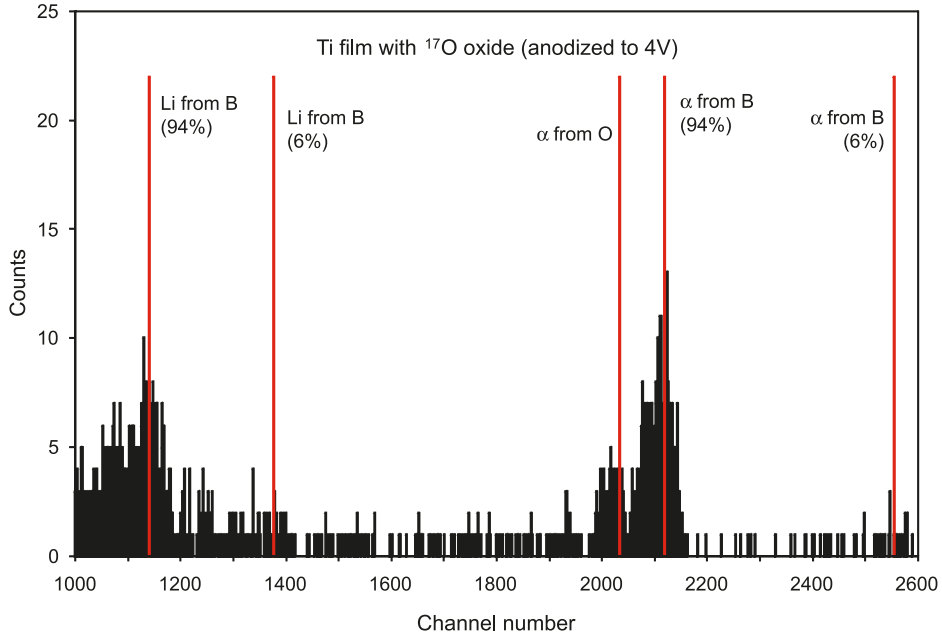

arising from the presence of ^{10}B and ^{17}O at a particular depth can be calculated. The result, obtained with the SRIM-2008 program [5], is shown in Fig. 5. The simulation assumes a detector with infinitely good energy resolution and three hypothetical cases: (*i*) if ^{17}O and ^{10}B were located right on the sample surface, i.e., at the TiO_2–vacuum interface (leading to δ-functions); (*ii*) at the Ti–TiO_2 interface (sharp peaks slightly down-shifted from the δ-functions); (*iii*) and finally at the Ti–Si interface (broader peaks further downshifted). The corresponding section of Fig. 3 has been overlaid with the simulated energy spectrum (the histogram), now plotted against α energy. We note that provided the two elements are located just at these interfaces, the two groups of peaks do not interfere with one another and would not even if we had folded in the 19 keV FWHM resolution of the actual detectors. Comparison with the histogram demonstrates that neither the oxide nor the metal layer is thick enough to cause enough downshift of α emission from ^{10}B to be in the region of the peak that we consider to be α from ^{17}O. According to further calculations, for the low-energy component of the double peak to be of B origin, the contaminant must lie as deep as 100 to 120 nm of Ti equivalent, i.e., well within the Si substrate. A double peak is not seen for the ^{16}O sample (Fig. 2), whose substrate is from the same batch as that of the ^{17}O sample. Hence the substrate is unlikely to be the origin of the double peak. All evidence then points to the conclusion that the lower energy peak of the double peak is indeed from ^{17}O.

Another check for the authenticity of the ^{17}O peak would be to closely analyze the peak originating from the recoil ^{7}Li of the boron reaction. The ^{7}Li particle count at 840 keV will match the 1472 keV α peak from the ^{10}B reaction one to one. In this trial demonstration, the poor statistics and electronic and (or) background noise prevented a definitive comparison.

Although not shown in the figures, a distinctive charged-particle peak was seen at low energies in the NDP spectra. The peak was later confirmed through repeated analysis of samples and standards to fall at about 584 keV, which strongly suggests the presence of nitrogen in the Ti film. The resolution is insufficient to determine if the nitrogen is in the Ti metal, oxide, or both. As TiN compounds do not readily form at room temperature, the nitrogen is thought to have been introduced during the Ti film deposition. The presence of residual nitrogen gas during the deposition process was likely because of the use of nitrogen gas in the regular operation of this particular equipment, i.e., not for our samples but for all other sample preparations.

We will finally comment on the likely source of boron contamination. Figure 5, along with the comparison of Figs. 2 and 3, suggest the Si substrates used were free of boron. Therefore the contamination occured during or after the sputtering process. In all figures, α particles originating from boron show little or no downshifting in energy: all cluster around 1472 keV and the width is consistent with the 18 keV FWHM resolution of the detector. Therefore, the contamination seems to be right on the surface or within the oxide layer. We note that boric acid is highly volatile. In hindsight, the borosilicate ampoules holding water (for both samples) should have been removed from the container to prevent continual volatilization of boric acid over the months of exposure.

5. Comparison of NDP withRBS and NRA

^{17}O being the only chemical species that could yield charged particles for detection (provided we succeed in eliminating boron), NDP provides a very clean signal. Indeed, due to the relatively weak flux of neutron beams and the small (n, α) cross-section, one might say it is too clean! The problem of a very weak signal can be overcome by installing more detectors. The all-important fact is that there are no intrinsic issues that will unavoidably lead to high background and (or) interference.

Fig. 5. Calculated spectrum of α particles escaping from a 49 nm thick Ti film deposited on Si substrate and covered by a 5 nm layer of TiO_2. Source of the particles is either ^{10}B or ^{17}O, hypothetically situated at three locations: (*i*) on the surface of the sample, (*ii*) at the Ti–TiO_2 interface, and (*iii*) at the Si–Ti interface. The three locations give rise to three peaks, respectively, appearing as δ-functions (for a detector with infinitely good energy resolution), as slightly downshifted sharp peaks, and much broader peaks at significantly lower energies. The histogram in the background is the double-peak feature of Fig. 3.

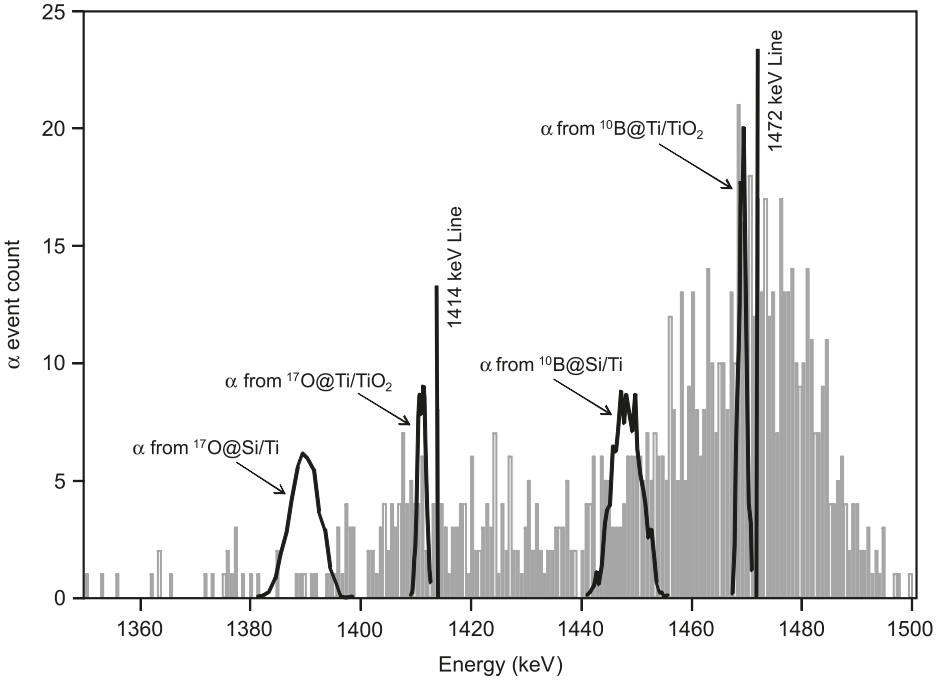

Mass resolution of ^{18}O and ^{16}O is definitely possible with RBS, as the kinematic factors for these isotopes differ significantly. A demonstration of this approach is seen in Fig. 1 of Christensen et al. [6], where the specially prepared sample is a Ti thin-film supported on a C substrate. Our simulations show that the same experiment on a >1 μm thick Ti sample would lead to difficulties in measuring small variations in oxygen peaks (oxygen content equivalent to $\sim 5 \times 10^{16}$atoms/cm^2) because of the high background. Assuming Rutherford cross-sections, we estimate that the integrated area for the oxygen peak for 5 nm thick TiO_2 will be ~90 times smaller compared with the background counts for a Ti substrate (for the same energy channels).

As for depth resolution, we note that the detectors used for NDP are exactly the same as those used for RBS or NRA. From this perspective, one expects exactly the same depth resolution derived from data of similar counting statistics. Most RBS and NRA spectra, when analyzed with a model, lead to a depth resolution of a few tens of nanometers when the sample and measuring conditions are fully optimized. Our results suggest a similar or a slightly smaller change in depth can be detected by NDP, even though our sample and experimental conditions were not so perfect. The anodization ratio of Ti is typically 2.5 nm/V. Since we anodized the sample to 4 V, the depth to the original ^{17}O oxide layer had increased, at most, by ~10 nm. As demonstrated above, the shift in the first moment of counts enabled us to detected this change.

Unlike RBS or NRA, that are part of the general arsenal of experimental techniques available to surface science, NDP works only with relatively few isotopes. It is a technique applicable only to certain niche situations, and study of passive oxides may be one of those situations. With its ability to investigate submicron oxide layers on any metal (regardless of *Z*) in any form (substrate-supported thin-film, foil, or plate) ^{17}O NDP could be a uniquely useful tool.

6. Conclusion

We have shown that ^{17}O NDP could become a powerful tool in the study of passive oxides. As expected, ubiquitous boron contamination is a serious threat. The problem is perhaps compounded by the fact that one is never far from glassware in a chemistry lab! However, the problem seems manageable and is likely to decrease as one gains experience. The following is a list of improvements that are likely to yield better results in the future:

(1) Better handling and storage of the samples, as well as more careful control of sample fabrication and (or) deposition conditions to prevent boron and nitrogen contamination.

(2) Because the neutron-induced charged particles travel isotropically from the reaction site, the majority of the available signal is lost to the chamber walls if only a small number of detectors are used. Currently, additional equipment is being acquired by NIST to install 8–10 additional charged-particle detectors. The additional detectors will give increased signal strength in direct proportion to the total solid angle covered by the detectors.

(3) Multiple detectors should be arranged in a geometry that will allow their counts to be summed. For example, the sample placed normal to the neutron beam could be viewed by a circular array of detectors forming a cone

of $\sim 90^\circ$ apex angle at the illuminated part of the sample. Two or several such cones with different apex angles will allow consistency checks, analogous to the $\sqrt{2}$ factor between our two detectors.

(4) Thicker metal films (or bulk metal samples such as a plate) will allow anodization to higher potentials. To address the point raised by Tun et al. 1999 [1], i.e., whether field-assisted ion transport or point defect model is at work in anodization of Ti, one needs to answer if the additional depth of ^{17}O is Δt or $(2/3)\Delta t$, where Δt is the thickening of the anodized oxide. Being able to grow thicker oxides will lead to a conclusion with higher confidence.

(5) Each ^{10}B reaction emits α and lithium particles in opposite directions, offering the following strategy to improve precision and detection limit for ^{17}O: Develop and experimentally test an algorithm to deduce the α-from-B spectrum from a measured recoil Li spectrum. One can then subtract the ^{10}B contribution from the measured α spectrum in the neighbourhood of the α-from-B peak, leading to determination of the purely ^{17}O α spectrum.

References

1. Z. Tun, J.J. Noël, and D.W. Shoesmith. J. Electrochem. Soc. **146**, 988 (1999). doi:10.1149/1.1391710.
2. Z. Tun, J.J. Noël, and D. Shoesmith. *In* Physics in Canada. Special issue on neutron and X-ray scattering at major facilities. *Edited by* J. Katsaras. Vol. 62. 2006. p. 249.
3. R.G. Downing, G.P. Lamaze, J.K. Langland, and S.T. Hwang. NIST J. Res. **98**, 109 (1993).
4. V.V. Andreeva. Corrosion, **20**, 35t (1964).
5. J.F. Ziegler. SRIM-2008, v. 2008.03. Available from http://www.srim.org.
6. N.S. Christensen, F. Jensen, F. Besenbacher, and I. Stensgaard. Nucl. Instrum. Methods Phys. Res. B, **51**, 97 (1990). doi:10.1016/0168-583X(90)90508-R.

List of symbols

CNBACK	Charged-particle detector that views sample at 42° angle
CNDAT	Charged-particle detector that views sample at 90° (normal to sample face)
CNDP	Cold-neutron depth profiling
n	Neutron
NDP	Neutron depth profiling
NIST	National Institute of Standards and Technology
R	Recoil nucleus
T	Target nucleus
α	Alpha particle
Δt	Thickening of anodized oxide
σ_a	Absorption cross-section for the (n, α) reaction